International Journal of Bridge Engineering (IJBE), Vol. 5, No. 3, (2017), pp. 01-23

# THE USE OF CLASSICAL ROLLING PENDULUM BEARINGS (CRPB) FOR VIBRATION CONTROL OF STAY-CABLES

Georgia Papastergiou[1]

[1] National Technical University of Athens, Dept. of Civil Engineering, Greece
e-mail: papastergiou.georgina@gmail.com

**ABSTRACT:** Cables are efficient structural elements that are used in cable-stayed bridges, suspension bridges and other cable structures. These cables are subjected to environmental excitations such as rain- wind induced vibrations. Rain-wind induced stay-cable vibrations may occur at different cable eigenfrequencies. Several methods, including aerodynamic or structural means, have been investigated in order to control the vibrations of bridge's stay-cables. Aerodynamic methods, such as modification of the cable roughness were effective only for certain types of vibration. Another method is the coupling of the stays with secondary wires, in order to reduce their effective length and thereby to avoid resonance. Finally, external transverse dampers have to be designed for several target cable modes in order to decrease the oscillations amplitude and to damping them. This paper investigates a movable anchorage system with a Classical Rolling Pendulum Bearing (CRPB) device. An analytical model of cable-damper system is developed herein based on the taut string representation of the cable. The gathered integral-differential equations are solved through the use of the Lagrange transformation. Finally, a case study with realistic geometrical parameters is also presented to establish the validity of the proposed system.

**KEYWORDS:** bridge dynamics; stay-cables; damping systems; bearings; vibration control

## 1 INTRODUCTION

Cable-stayed (C-S) bridges have been known since the beginning of the 18$^{th}$ century, but they have been of great interest only in the last sixty years, particularly due to their special shape and also because they are an alternative solution to suspension bridges for long spans. The main reasons for this delay were the difficulties in their static and dynamic analysis, the various nonlinearities, and the absence of computational capabilities, the lack of high strength materials and the lack of construction techniques. There are numerous

studies dealing with the static behavior, the dynamic analysis, and the stability of C-S bridges. The static behavior of C-S bridges is described in the works of Fleming [1], Kollbruner et al [2], Bruno and Grimaldi ([3], Gimsing [4], Khalil [5], Virgoreux [6], Michaltsos et al [7] and Freire et al [8], while dynamical analyses of C-S bridges can be found in the works of Fleming and Egeseli [9], Nazmy and Abdel-Ghaffar [10], Abdel-Ghaffar and Khalifa [11], Bruno and Colotti [12], Chatterjee et al [13], Michaltsos [14], Konstantakopoulos et al [15], Wang et al [16], Cao et al [17], Macdonald [18], and Raftoyiannis and Michaltsos [19]. Stability aspects of C-S bridges are presented in the book by Raftoyiannis and Michaltsos [20] as well as in the works of Ermopoulos et al [21], Bosdogianni and Olivari [22], Michaltsos [23], Michaltsos et al [24] and Pedro and Reis [25].

A significant problem, which arose from the practice, is the cables rain-wind induced vibrations. Large amplitude Rain-Wind-Induced-Vibrations (RWIV) of stay-cables constitutes a challenging problem in the design of C-S bridges. Such phenomena were first observed on the Meikonishi bridge in Nagoya-Japan by Hikami and Shiraishi [26] and also later on other similar bridges, as for instance the steel Erasmus bridge in Rotterdam-Netherlands by Achkire and Preumont [27] and the Second Severn Crossing, connecting England and Wales by Macdonald et al. [28]. It was found that the cables, which were stable under wind action only, were oscillating under a combined influence of rain and wind, leading to large amplitude motions, even for light-to-moderate simultaneous rain and wind action. The frequency of the observed vibrations was much lower than the critical one of the vortex-induced vibrations, while it was also perceived that the cable oscillations took place in the vertical plane mostly in single mode; for increasing cable length however, higher modes (up to the 4th) appeared. Most importantly, during the oscillations a water rivulet appeared on the lower surface of the cable, which was characterized by a leeward shift and vibrated in circumferential directions as described in the works of Wilde and Witkowski [29], Ibrahim [30], and Sophianopoulos [31]. The so-produced vibrations may result in a reduced life of the cable and its connection due to fatigue or rapid progress of the corrosion.

Several methods, including aerodynamic or structural techniques, have been investigated in order to control the vibrations of bridge's stay cables. Aerodynamic methods, such as modification of the cables' roughness were effective only for certain types of vibration. Another method is the coupling of the stays with secondary wires, in order to reduce their effective length and thereby to avoid resonance. This method affects the bridge's aesthetics. Finally, external transverse dampers have to be designed for several target cable modes in order to decrease the oscillations amplitude and to damping them.

In C-S bridges, the stays are generally fixed in anchorages on the deck through an anchor head as shown in Fig.1.

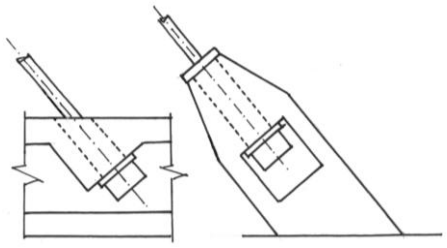

*Figure 1.* Anchorage of stays

This paper investigates the effectiveness of a movable anchorage system with a Classical Rolling Pendulum Bearing (CRPB) device. An analytical model of the cable-damper system is developed herein based on the taut string representation of the cable. The gathered integral-differential equations are solved through the use of the Lagrange transformation. Finally, a case study with realistic geometrical parameters is also presented to establish the validity of the proposed system, while the required device for the studied case is designed. It must be reminded that this solution, with various forms (see Fig. 2) was described, patented, and finally used by Jules Touaillon [32].

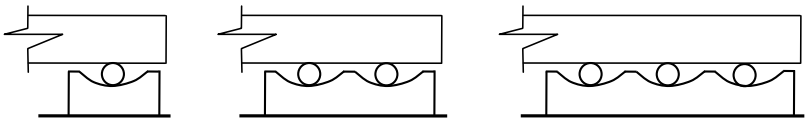


*Figure 2.* Various forms of a CRPB with: (a) one, (b) two, and (c) three concaves

## 2 BASIC ASSUMPTIONS

a) The deformed shape of the cables under dead and live loads is a catenary curve, with displacements $w_o$ and tensile forces $T_o$ (see Fig.3), which because of its very shallow form can be approximated by a second-order parabola.
b) Under the action of the dynamic loads $p_y(x,t)$ and $p_z(x,t)$, the cable takes the form of Fig. 4, with additional displacements $u_d$, $\upsilon_d$, $w_d$ and tensile forces $T_d$.
c) The static and dynamic tensile forces are related as follows:

$$\left.\begin{aligned} T(t) &= T_o + T_d(t) \\ H(t) &= H_o + H_d(t) \end{aligned}\right\} \qquad (1)$$

where H, is the projection of force T on x-axis.

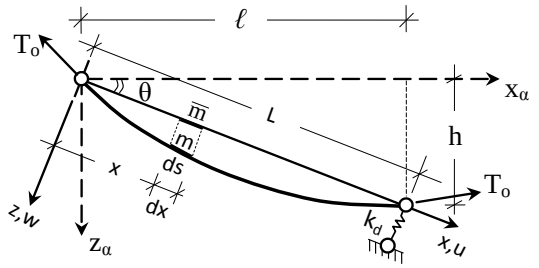


*Figure 3.* Cable and reference axes

d) The masses $\overline{m}(x)$ and $m(s)$ shown in Fig. 3, are related through the expression

$$\overline{m}(x) = m(s)\frac{ds}{dx} \qquad (2)$$

e) The studied cables are referred to the inclined axis system 0-xyz of Figs. 3 and 4.

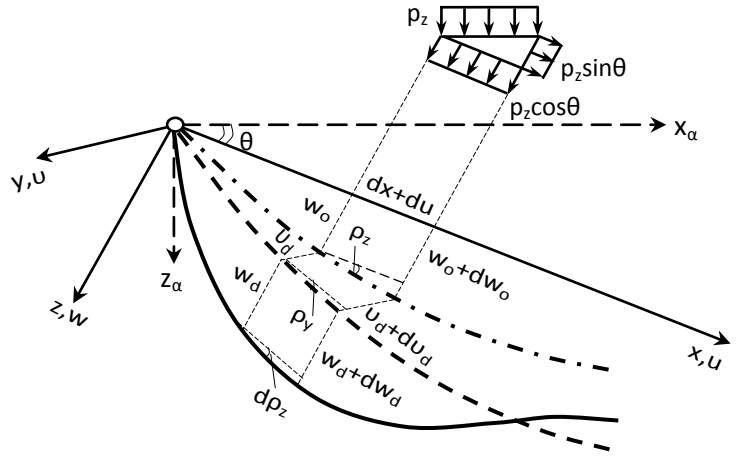


*Figure 4.* Deformation of the cable

## 3 EQUILIBRIUM EQUATIONS OF A TAUT CABLE

In this section, the equations governing the behavior of a taut cable, the one end of which is movable (see Fig. 4), are derived.

### 3.1 Projection on xoz-plane

For a shallow form of the cable, the following relations are valid:

$$\left.\begin{aligned} &\cos\rho_z = dx/ds \cong 1 \\ &\sin\rho_z = dw/ds \\ &\sin d\rho_z \cong 0 \end{aligned}\right\} \qquad (3)$$

### *3.1.1 Equilibrium of horizontal forces*

Projecting on xoz-plane and taking the equilibrium of horizontal forces, we obtain:

$$-T\frac{dx}{ds} + T\frac{dx}{ds} + \partial\left(T\frac{dx}{ds}\right) + p_x ds - c\dot{u}ds - m\ddot{u}ds = 0\,, \qquad \text{or finally:}$$

$$\frac{\partial H}{\partial s} - c\dot{u} - m\ddot{u} = -p_x(x,t) \qquad (4)$$

### *3.1.2 Equilibrium of vertical forces*

Projecting on xoz-plane and taking the equilibrium of vertical forces, we obtain:

$$-T\frac{\partial w}{\partial s} + T\frac{\partial w}{\partial s} + \partial\left(T\frac{\partial w}{\partial s}\right) + \overline{m}gds + p_z ds - c\dot{w}ds - m\ddot{w}ds = 0 \qquad (5a)$$

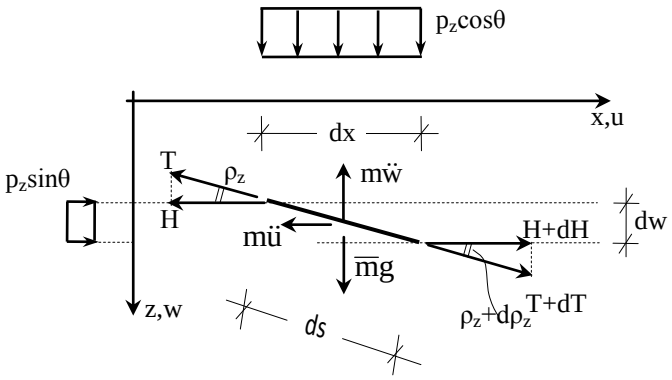


*Figure 5.* Projection on xoz-plane

Taking into account the equation of static equilibrium, i.e.,

$\frac{\partial}{\partial s}(T_o\frac{\partial w_o}{\partial s}) = -\overline{m}g$, and that are also valid: $w = w_o + w_d$ and $\frac{\partial w_o(x)}{\partial t} = 0$

equation (5a) becomes:

$$T_o\frac{\partial^2 w_d}{\partial x^2} + T_d\left(\frac{\partial^2 w_o}{\partial x^2} + \frac{\partial^2 w_d}{\partial x^2}\right) - c\dot{w}_d - m\ddot{w}_d = -p_z(x,t) \qquad (5b)$$

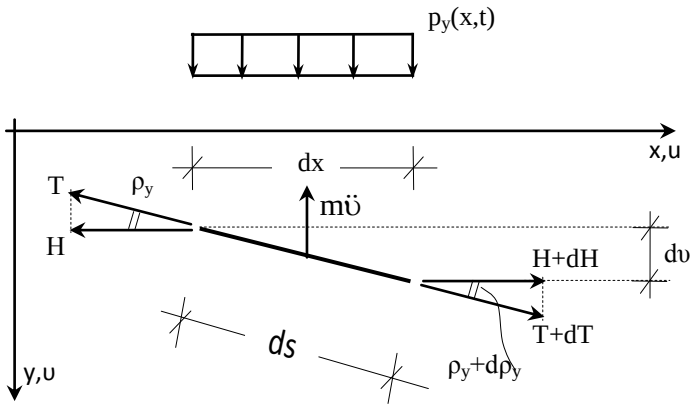


*Figure 6.* Projection on xoy-plane

### 3.2 Projection on xoy-plane

Projecting on xoy-plane, taking the equilibrium of vertical forces, and through a similar process like the one of §3.1, we obtain:

$$T_o \frac{\partial^2 \upsilon_d}{\partial x^2} + T_d \frac{\partial^2 \upsilon_d}{\partial x^2} - c\dot{\upsilon}_d - m\ddot{\upsilon}_d = -p_y(x,t) \tag{6}$$

### 3.3 The cables' deformation

The following relations are valid:

$$\left.\begin{aligned} ds^2 &= dx^2 + dw_o^2 \\ (ds+\Delta ds)^2 &= (dx+\Delta dx)^2 + (\Delta d\upsilon)^2 + (dw_o + \Delta dw_o)^2 \end{aligned}\right\} \tag{7}$$

From the second of eq (7), neglecting the higher order terms we get: $\Delta dx = \Delta ds \frac{ds}{dx} - \Delta dw_o \frac{dw_o}{dx}$, and taking into account that $\Delta dw_o = dw_d$, we obtain:

$$\Delta dx = \frac{\Delta ds}{ds} \cdot \frac{ds}{dx} \cdot \frac{ds}{dx} dx - \frac{dw_d}{dx} \cdot \frac{dw_o}{dx} dx \tag{8}$$

On the other hand, we know that: $\sigma = \varepsilon \cdot E$ or

$$\varepsilon = \frac{\sigma}{E} = \frac{T_d}{EA} \tag{9a}$$

Because of eq(9a), eq(8) becomes: $\Delta dx = \frac{T_d}{EA} \cdot \left(\frac{ds}{dx}\right)^2 \cdot dx - \frac{dw_d}{dx} \cdot \frac{dw_o}{dx} \cdot dx$ and

using the condition $\int_0^L \Delta dx = 0$, the above gives:

$$\frac{T_d}{EA}\int_0^L \frac{dx}{\cos^3 \rho_z} - \int_0^L \frac{dw_d}{dx}\cdot\frac{dw_o}{dx}\cdot dx = 0 \qquad (9b)$$

From this last, after integration by members and with boundary condition $w_d(0) = 0$ we obtain:

$$\left.\begin{aligned} T_d &= \frac{1}{L_o}\left( w_o'(L)w_d(L) - w_o''\int_0^L w_d dx \right) \\ \text{with: } L_o &= \int_0^L \frac{dx}{EA\cos^3\rho_z} \end{aligned}\right\} \qquad (10)$$

## 3.4 Catenary and the parabola approach

It is necessary to determine the form of a cable in rest, i.e. $w_o$. In this case, we have: $p_z(x,t) = p_y(x,t) = 0$, $u = \upsilon = 0$, $w = w_o(x)$.

Therefore, equation (4) gives: $\frac{\partial H_o}{\partial s} = 0$, which results

$$H_o = \text{constant} \qquad (11)$$

On the other hand, equation (5a) gives: $\frac{\partial}{\partial s}\left( T_o \frac{\partial w_o}{\partial s} \right) = -\overline{m}g$ or

$\frac{\partial}{\partial s}\left( T_o \cdot \frac{dx}{ds}\cdot\frac{dw_o}{dx} \right) = \frac{\partial}{\partial s}\left( H_o \cdot \frac{dw_o}{dx} \right) = -\overline{m}\cdot g$, or finally:

$$H_o \cdot \frac{d^2 w_o}{dx^2} = -\overline{m}\cdot g = -m\cdot g\cdot\frac{ds}{dx} \qquad (12)$$

It is usual to use the parabola as a curve that is very close to the catenary one, especially for shallow forms of cables. For a cable's shallow form (i.e. $ds \approx dx$), the equation of a parabola passing from the points (0,0), (L,0) and having $w_o'' = -\frac{\overline{m}g}{H_o}$ (from eq. 12), is given by the following formula:

$$w_o(x) = \frac{\overline{m}g}{2H_o}\cdot x\cdot(L-x) \qquad (13)$$

A comparison between the parabolic form of a cable (as the used in C-S Bridges) and the catenary one shows that the differences of the two curves' sags amount up to 0.02%.

# 4 ANALYSIS

## 4.1 The cable

In C-S-bridges, stay cables are generally fixed in anchorages on the deck through a socket or an anchor-head as shown in Fig. 1.
The stay-cable model with the considered anchorage-bearing system is shown in Fig. 7.

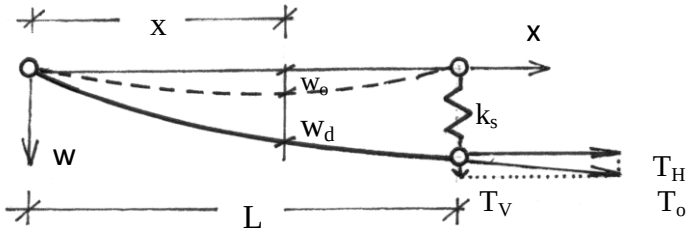


*Figure 7.* The stay-cable model

For small deflections, according to §3, the motion of the cable is described by the following equation:

$$\left.\begin{aligned} &T_o w_d'' + T_d w_o'' - c\dot{w}_d - m\ddot{w}_d = p(x,t) + F_H \cdot \delta(x-L) \\ &T_d = \frac{w_o'(L) w_d(L)}{L_o} - \frac{w_o''}{L_o}\int_0^L w_d\,dx \end{aligned}\right\} \qquad (14a,b)$$

with: $L_o = \int_0^L \frac{dx}{EA\cos^3\rho_z}$ and boundary conditions:

$$\left.\begin{aligned} &w_d(0) = 0 \\ &T_o w_d'(L) + k_s w_d(L) = 0 \end{aligned}\right\} \qquad (15a,b)$$

where $F_H$ is the acting force due to the bearing device and $\delta$ the Dirac delta function.

## 4.2 The rolling pendulum bearing system

Let us consider a C.R.P.B. device with one concave rolling, like the one of Fig.8. The C.R.P.B. system is made from material like the one of the classical ball-bearings (see also paragraph 6), having surfaces elaborated wery diligently, with coefficient of rolling friction ranging from 0.002 to 0.005. Therefore, the developed friction forces can be neglected in this preliminary study. On the other hand, the angle of the friction cone amounts up to $0.34^o$, which corresponds to a very small static friction.

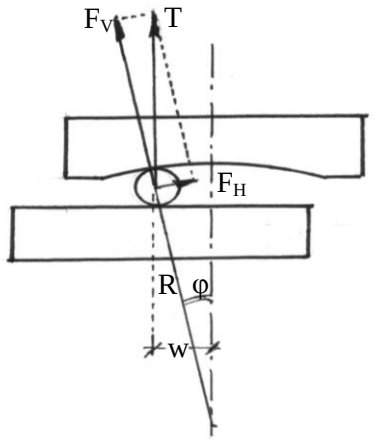


*Figure 8.* Geometry of a C.R.P.B. system

For very small values of the angle φ, it is:

$$\left.\begin{aligned}\cos\varphi &= 1\\ \tan\varphi &= \frac{w_L}{R}\end{aligned}\right\} \qquad (16a,b)$$

Equilibrium of forces gives:

$$F_H = T_o \tan\varphi = T_o \frac{w_L}{R} \qquad (17)$$

Moreover, we have $k_S = \frac{F_H}{w_L}$, which because of eq(17) gives:

$$k_S = \frac{T_o}{R} \qquad (18)$$

### 4.3 The rolling pendulum bearing system

Introducing eq(14b) into eq(14a) and taking into account eqs (17) and (18), we obtain the following equation of motion:

$$\left.\begin{aligned}&T_o w_d'' + \frac{w_o'(L) w_d(L)}{L_o} w_o'' - \frac{w_o''^2}{L_o}\int_0^L w_d dx - c\dot{w}_d - m\ddot{w}_d = p(x,t) + \frac{T_o}{R} w_d \delta(x-L)\\ &\text{with boundary conditions:} \quad w_d(0) = 0\\ &\qquad\qquad \text{and} \quad T_o w_d'(L) + \frac{T_o}{R} w_d(L) = 0\end{aligned}\right\} \qquad (19)$$

### 4.4 The free vibrating cable

The equation of motion of a free vibrating cable with movable anchorage is:

$$T_o w_d'' - c\dot{w}_d - m\ddot{w}_d = -\frac{w_o'(L)w_d(L)}{L_o} w_o'' + \frac{w_o''^2}{L_o}\int_0^L w_d dx \tag{20}$$

We are searching for a solution of separated variables of the form:

$$w_d(x,t) = W(x)\Phi(t) \tag{21}$$

Introducing eq(21) into eq(20) we get:

$$\frac{T_o W'' + \frac{w_o'(L)w_o''}{L_o} W(L) - \frac{w_o''^2}{L_o}\int_0^L W dx}{mW} = \frac{\ddot{\Phi} + \frac{c}{m}\dot{\Phi}}{\Phi} = -\omega^2$$

which concludes to the following uncoupled equations:

$$\left.\begin{aligned} &W'' + \frac{m\omega_w^2}{T_o} W = -\frac{w_o'(L)w_o''}{L_o T_o} W(L) + \frac{w_o''^2}{T_o L_o}\int_0^L W dx \\ &\ddot{\Phi} + \frac{c}{m}\dot{\Phi} + \omega_w^2 \Phi = 0 \end{aligned}\right\} \tag{22}$$

The above integral-differential equation (22) has the solution:

$$\left.\begin{aligned} &W(x) = c_1 \sin\lambda x + c_2 \cos\lambda x - \frac{w_o'(L)w_o''}{\lambda^2 L_o T_o} W(L) + \frac{w_o''^2}{\lambda^2 T_o L_o}\int_0^L W dx \\ &\text{with:}\quad \lambda^2 = \frac{m\omega^2}{T_o} \end{aligned}\right\} \tag{23}$$

Setting x=L, the above eq(23), becomes:

$W(L) = c_1 \sin\lambda L + c_2 \cos\lambda L - \frac{w_o'(L)w_o''}{\lambda^2 L_o T_o} W(L) + \frac{w_o''^2}{\lambda^2 T_o L_o}\int_0^L W dx$, which finally gives:

$$W(L) = \frac{\lambda^2 L_o T_o}{\lambda^2 L_o T_o + w_o'(L) w_o''} \cdot \left( c_1 \sin\lambda L + c_2 \cos\lambda L + \frac{w_o''^2}{\lambda^2 L_o T_o}\int_0^L W dx \right) \tag{24}$$

Because of eq(24), eq(23) becomes:

$$\left.\begin{aligned} &W(x) = c_1(\sin\lambda x + G_1\sin\lambda L) + c_2(\cos\lambda x + G_1\cos\lambda L) + (G_2 + G_3) + \int_0^L W dx \\ &\text{where:}\quad G_1 = \frac{w_o'(L)w_o''}{\lambda^2 L_o T_o + w_o'(L)w_o''},\quad G_2 = \frac{w_o''^2}{\lambda^2 L_o T_o},\quad G_3 = G_1 \cdot G_2 \end{aligned}\right\} \quad (25)$$

Equation (25), which is of Hammerstein type, gives after integration:

$$\int_0^L W dx = \frac{1}{1-(G_2+G_3)L} \cdot \left\{ c_1\left(\frac{1-\cos\lambda L}{\lambda} + G_1 L\sin\lambda L\right) + c_2\left(\frac{\sin\lambda L}{\lambda} + G_1 L\sin\lambda L\right)\right\}$$

Therefore, equation (25) becomes:

$$\left.\begin{aligned} &W(x) = c_1(\sin\lambda x + D_1) + c_2(\cos\lambda x + D_2) \\ &\text{where:}\quad D_1 = G_1\sin\lambda L + \frac{G_2+G_3}{1-(G_2+G_3)}\left(\frac{1-\cos\lambda L}{\lambda} + G_1 L\sin\lambda L\right) \\ &\qquad\quad D_2 = G_1\cos\lambda L + \frac{G_2+G_3}{1-(G_2+G_3)}\left(\frac{\sin\lambda L}{\lambda} + G_1 L\cos\lambda L\right) \end{aligned}\right\} \quad (26)$$

Introducing equation (26) into the boundary conditions of eq(19) we obtain:

$$\left.\begin{aligned} &c_1 D_1 + c_2(1+D_2) = 0 \\ &c_1\left[\lambda T_o\cos\lambda L + \frac{T_o}{R}(\sin\lambda L + D_1)\right] + c_2\left[-\lambda T_o\sin\lambda L + \frac{T_o}{R}(\cos\lambda L + D_2)\right] = 0 \end{aligned}\right\} \quad (27)$$

In order for the above system to have a non-trivial solution, the determinant of the coefficients of the unknowns must be zero. This condition concludes to the following eigenfrequencies' equation:

$$D_2\left[D_1 - (1+D_2)\frac{T_o}{R}\right] + \left[D_1\frac{T_o}{R} - (1+D_2)T_o\lambda\right]\cos\lambda L - \left[(1+D_2)\frac{T_o}{R} + D_1 T_o\lambda\right]\sin\lambda L = 0 \quad (28)$$

Finally from equations (27), (28) and the first of (26), one can determine the following form of the shape functions:

$$W_n(x) = c_1\left[(\sin\lambda_n x + D_1) + \frac{\lambda_n T_o \cos\lambda_n L + \frac{T_o}{R}(\sin\lambda_n L + D_2)}{\lambda_n T_o \sin\lambda_n L - \frac{T_o}{R}(\cos\lambda_n L + D_2)} \cdot (\cos\lambda_n x + D_2)\right] \tag{29}$$

## 4.5 The forced vibrating cable

The forced vibration of a stay-cable, is described by equation (19) of §4.3:

$$T_o w_d'' + \frac{w_o'(L) w_d(L)}{L_o} w_o'' - \frac{w_o''^2}{L_o}\int_0^L w_d dx - c\dot{w}_d - m\ddot{w}_d = p(x,t) + \frac{T_o}{R} w_d \delta(x-L)$$

We are searching for a solution of the form:

$$w_d(x,t) = \sum_n W_n(x) Z_n(t) \tag{30}$$

where $W_n(x)$ is taken from eq(29) and $Z_n(t)$ unknown time functions under determination. Introducing eq(30) into the first of (19), we get:

$$\left.\begin{aligned} T_o\sum_n W_n'' Z_n + \frac{w_o'(L) w_o''}{L_o}\sum_n W_n(L) Z_n - \frac{w_o''^2}{L_o}\int_o^L \sum_n W_n Z_n dx - c\sum_n W_n \dot{Z}_n - m\sum_n W_n \ddot{Z}_n = \\ = p_z(x) f(t) + \frac{T_o}{R}\sum_n W_n Z_n\ \delta(x-L) \end{aligned}\right\} \tag{31}$$

Since $W_n$ satisfies the first of eq(22), the above becomes:

$$\left.\sum_n \omega_n^2 W_n Z_n + \frac{c}{m}\sum_n W_n \dot{Z}_n + \sum_n W_n \ddot{Z}_n = \frac{p_z(x) f(t)}{m} + \frac{T_o}{mR}\sum_n W_n Z_n \delta(x-L)\right\} \tag{32}$$

Multiplying by $W_k$, and integrating the outcome from 0 to L, we finally obtain:

$$\left.\begin{aligned} \ddot{Z}_k + \frac{c}{m}\dot{Z}_k + \omega_k^2 Z_k = \frac{f(t)\int_0^L p_z(x) W_k dx}{m\int_0^L W_k^2 dx} + \frac{T_o}{R}\cdot\frac{W_k(L)\sum_n W_n(L) Z_n}{m\int_0^L W_k^2 dx} \\ \text{for:}\quad k = 1 \quad \text{to} \quad n \end{aligned}\right\} \tag{33}$$

In order to solve the above differential system, we use the Lagrange transformation. Therefore, we set:

$$\left.\begin{aligned} LZ_k(t) = \zeta_k(s) \\ Lf(t) = F(s) \end{aligned}\right\} \tag{34a,b}$$

and with initial conditions:

$$Z_k(0) = \dot{Z}_k(0) = 0 \qquad (35a,b)$$

we conclude to the following system:

$$\left.\begin{aligned}
&\alpha_{k1}\zeta_1 + \alpha_{k2}\zeta_2 + \cdots\cdots + \alpha_{kn}\zeta_n = \beta_k \quad , \qquad \text{where:} \\
&\alpha_{k\rho} = -\frac{T_o}{R}\cdot\frac{W_k(L)W_\rho(L)}{m\int_0^L W_k^2 dx} \ , \\
&\alpha_{kk} = s^2 + \frac{c}{m}\cdot s + \omega_k^2 - \frac{T_o}{R}\cdot\frac{W_k^2(L)}{m\int_0^L W_k^2 dx} \ , \\
&\beta_k = \frac{\int_0^L p_z(x)W_k dx}{m\int_0^L W_k^2 dx}\cdot F(s) \\
&k = 1 \text{ to } n, \quad \rho = 1 \text{ to } n
\end{aligned}\right\} \qquad (36)$$

From the solution of the above system, we obtain $\zeta_k$ , and finally:

$$Z_k(t) = L^{-1}\zeta_k(s) \qquad (37)$$

## 5 NUMERICAL RESULTS AND DISCUSSION

### 5.1 The Cables

Let us consider a C-S bridge with dense distribution of cables from which we study a cable having tension $T_o$=300000 dN/cable, cross-sectional area $F=7.5\cdot10^{-3}m^2$, diameter D=0.13 m, weight G=70 dN/m, mass per unit length m=7kg/m, and variable length L=150, 250, and 350m.

### 5.2 The rain-wind combination

It has been observed that the rain-wind-induced vibration in bridge cables usually occurs in a frequency range from 0.5 to 4 $sec^{-1}$. For the study of the vibration of a cable under the action of a rain-wind combination we choose the following loading: $p = p(x)\cdot f(t) = 20\cdot\sin\omega t$ , where ω= 1, 2, 3, 4 $sec^{-1}$ (for the study of the above cables without a damping system) and ω= 3 $sec^{-1}$ (for the study of the above cables with the proposed C.R.P.B. devise).

### 5.3 Behavior of the cables without a damping system

Using equation (9.9) with $T_o/R = \infty$, we determine the eigenfrequencies of the

above considered cables, as they are shown in the following Table 1.

*Table 1*. Eignefrequencies of the cables

| | m=7kg/m , $T_o$=300000 dN | | |
|---|---|---|---|
| | L=150m | L=250m | L=350m |
| $\omega_1$ | 4.4697 | 2.8186 | 2.1507 |
| $\omega_2$ | 8.6716 | 5.2029 | 3.7164 |
| $\omega_3$ | 13.0125 | 7.8130 | 5.5868 |
| $\omega_4$ | 17.3432 | 10.4059 | 7.4328 |
| $\omega_5$ | 21.6801 | 13.0093 | 9.2936 |

In Figs 9 to 11, one can see the oscillations of the mid-length of the studied cables with length L=150, L=250 and L=350m, subjected to loadings acting with frequencies $\omega$=1, 2, 3, 4 $sec^{-1}$.

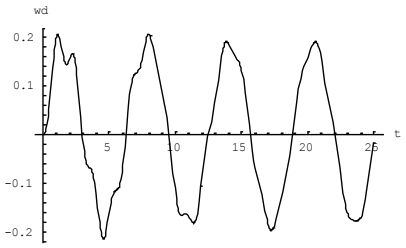


p=20·Sin(1·t)

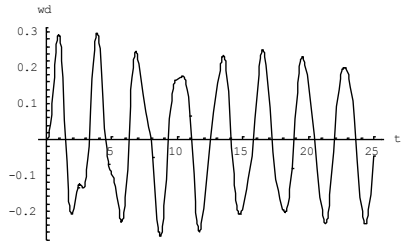


p=20·Sin(2·t)

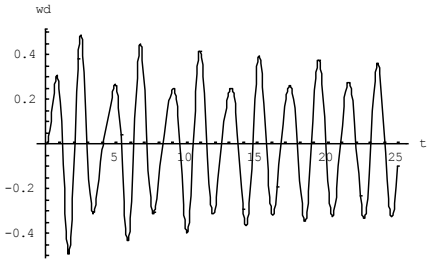


p=20·Sin(3·t)

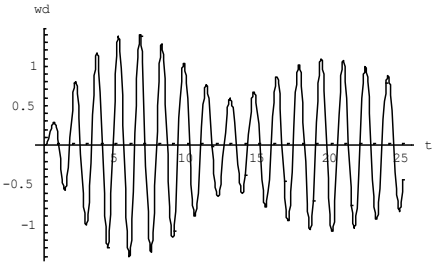


p=20·Sin(4·t)

In this case, big deformations appear, because the eigenfrequency of the external load near to the first one of the cable ( $\omega_1$ =4.47 $sec^{-1}$)

*Figure 9.* Oscillations of the mid-length of a cable of length L=150m, without any damping system

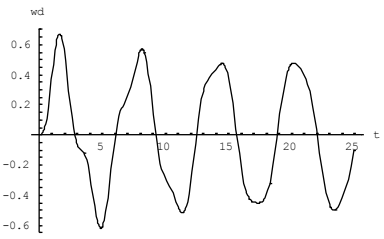


p=20·Sin(1·t)

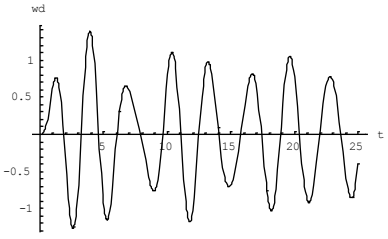


p=20·Sin(2·t)

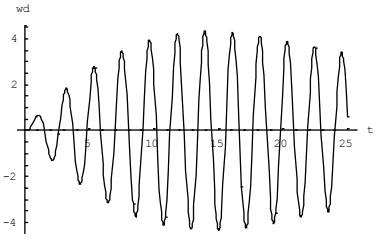


p=20·Sin(3·t)

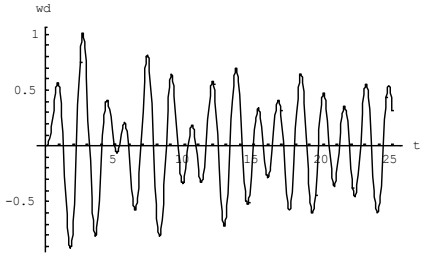


p=20·Sin(4·t)

In this case, big deformations appear, because the eigenfrequency of the external load is near tothe first one of the cable ($\omega_1$ =2.82 sec$^{-1}$).

*Figure 10.* Oscillations of the mid-length of a cable of length L=250m, without any damping system.

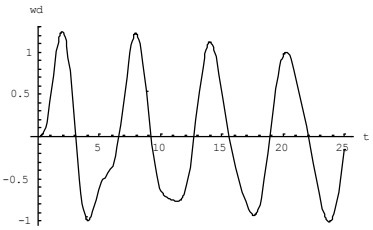


p=20·Sin(1·t)

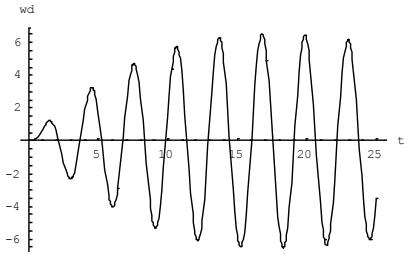


p=20·Sin(2·t)

In this case, big deformations appear, because the eigenfrequency of the external load is near to the first one of the cable ($\omega_1$ =2.15 sec$^{-1}$).

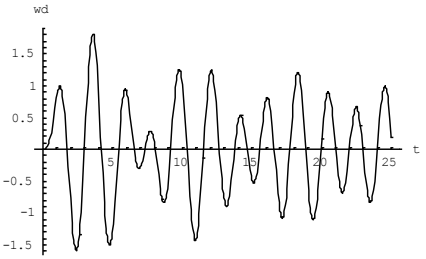


p=20·Sin(3·t)

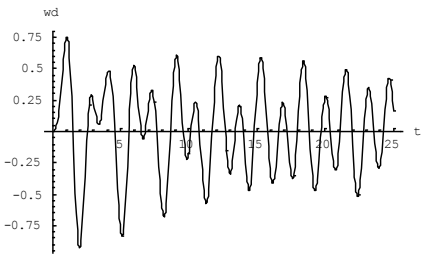


p=20·Sin(4·t)

*Figure 11.* Oscillations of the mid-length of a cable of length L=350m, without any damping system

## 5.4 The damping system

In the followings, we will use a C.R.P.B. device, based on the operation principle of the simple system of Fig. 8 and which will be designed in detail in the next paragraph 6.
We will consider devices with concave radii R=1, 2, and 3 meters.
The corresponding eigenfrequencies of a cable supplied by such a device are given in the following Table 2 (using eq. 9).

*Table 2.* Eigenfrequencies of cables with respect to concave radius R

| L | 150 | | | | 250 | | | | 350 | | | |
|---|---|---|---|---|---|---|---|---|---|---|---|---|
| R | 3 | 2 | 1 | ∞ | 3 | 2 | 1 | ∞ | 3 | 2 | 1 | ∞ |
| $\omega_1$ | 4.365 | 4.393 | 4.420 | 4.470 | 2.739 | 2.749 | 2.758 | 2.817 | 2.046 | 2.051 | 2.057 | 2.151 |
| $\omega_2$ | 8.518 | 8.573 | 8.628 | 8.672 | 5.166 | 5.185 | 5.190 | 5.203 | 3.698 | 3.701 | 3.712 | 3.716 |
| $\omega_3$ | 12.762 | 12.845 | 12.930 | 13.012 | 7.726 | 7.756 | 7.787 | 7.813 | 5.546 | 5.562 | 5.578 | 5.587 |
| $\omega_4$ | 17.014 | 17.121 | 17.232 | 17.343 | 10.290 | 10.330 | 10.370 | 10.406 | 7.379 | 7.399 | 7.420 | 7.433 |
| $\omega_5$ | 21.268 | 21.400 | 21.539 | 21.680 | 12.859 | 12.909 | 12.960 | 13.009 | 9.218 | 9.244 | 9.271 | 9.294 |

In the plots of Figs 12, 13, 14, we see the oscillations of the middle and of the anchor head of a cable of length 150m, tension 300000dN, and for different values of R.

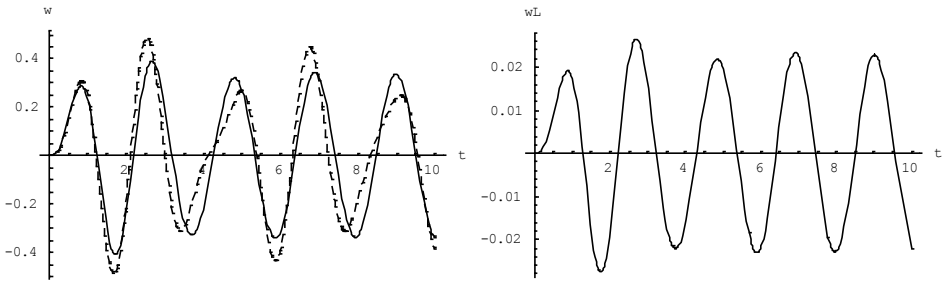


*Figure 12.* Oscillations of the mid-length and of its anchor head of a cable of L=150m, R=3m
___ with C.R.P.B. - - - without C.R.P.B

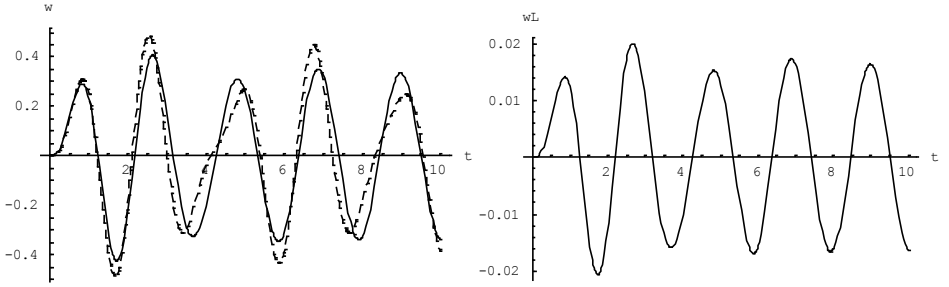


*Figure 13.* Oscillations of the mid-length and of its anchor head of a cable of L=150m, R=2m
___ with C.R.P.B. - - - without C.R.P.B

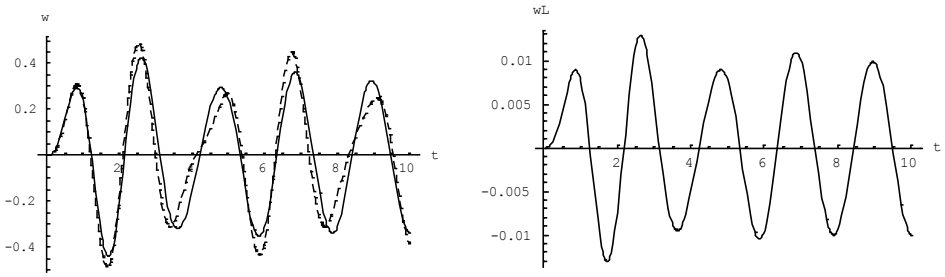


*Figure 14.* Oscillations of the mid-length and of its anchor head of a cable of L=150m, R=1m
___ with C.R.P.B. - - - without C.R.P.B

From the above plots of Figs 12 to 14, we ascertain that smaller radii are more effective than the greater ones. The above results are valid for both the cables' deformations and the anchorages' motion.
In the plots of Figs 15, 16, and 17, we see the oscillations of the mid-length and of the anchor head of a cable of length 250m, tension 300000dN, and for different values of R.

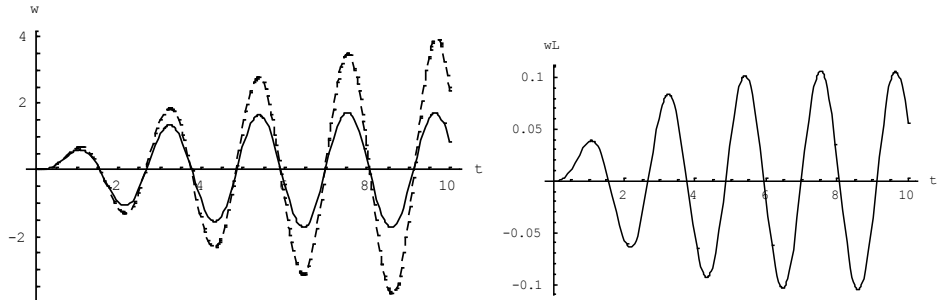


*Figure 15.* Oscillations of the mid-length and of its anchor head of a cable of L=250m, R=3m
___ with C.R.P.B. - - - without C.R.P.B

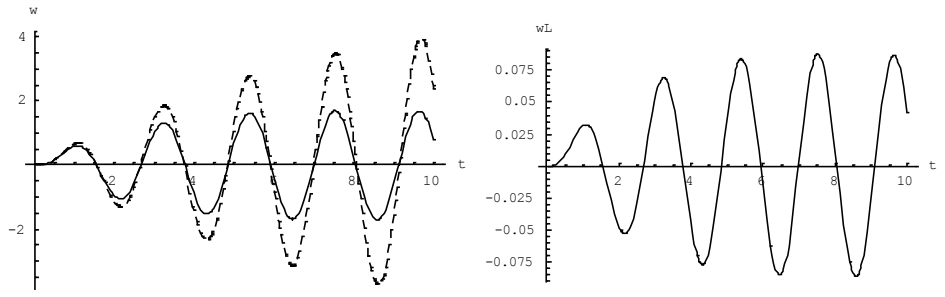


*Figure 16.* Oscillations of the mid-length and of its anchor head of a cable of L=250m, R=2m
___ with C.R.P.B. - - - without C.R.P.B

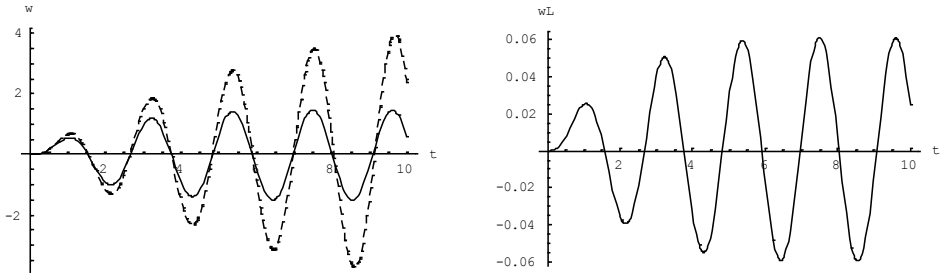


*Figure 17.* Oscillations of the mid-length and of its anchor head of a cable of L=250m, R=1m
___ with C.R.P.B. - - - without C.R.P.B

From the above plots of Figs 15 to 17, we observe that although the oscillations' amplitude is remarkable large (because the frequency of the external loading approaches the first eigenfrequency of the cable) the effectiveness of the system is obvious. We ascertain, again, that smaller radii are more effective than the greater ones. The above results are valid for both the cables' deformations and the anchorages' motion. In the plots of Figs 18, 19, and 20, we see the oscillations of the mid-length and of the anchor head of a cable with length 350m, tension 300000dN, and for different values of R.

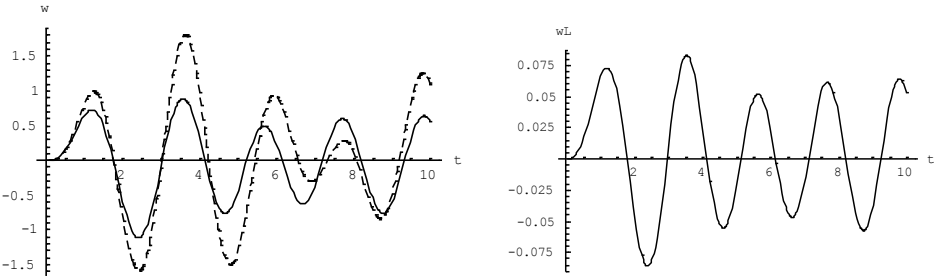


*Figure 18.* Oscillations of the mid-length and of its anchor head of a cable of L=350m, R=3m
___ with C.R.P.B. - - - without C.R.P.B

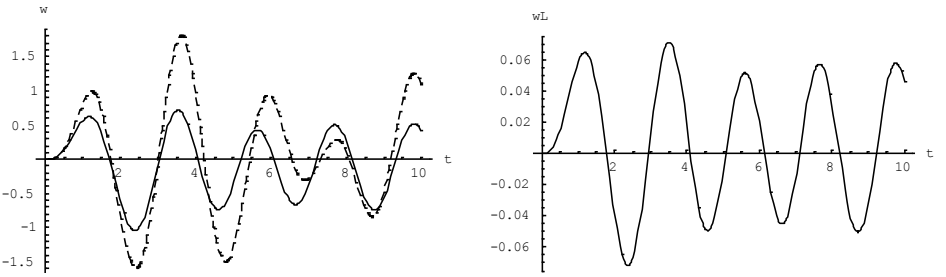


*Figure 19.* Oscillations of the mid-length and of its anchor head of a cable of L=350m, R=2m
___ with C.R.P.B. - - - without C.R.P.B

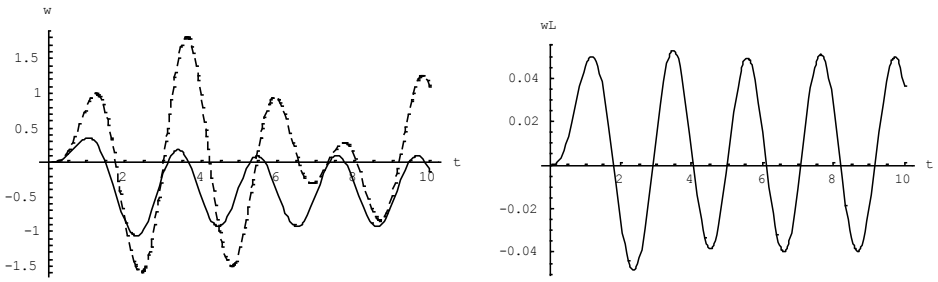


*Figure 20.* Oscillations of the mid-length and of its anchor head of a cable of L=350m, R=1m
___ with C.R.P.B. - - - without C.R.P.B

From the above plots of Figs 18 to 20, we ascertain, once again, that smaller radii are more effective than the greater ones. The above results are valid for both the cables' deformations and the anchorages' motion.

## 6 DESIGN OF A C.R.P.B. DEVICE

### 6.1 Bearing capability

Manufactures of ball bearings typically publish "LOAD RATINGS" for each bearing that they produce. The methods used to calculate loads, is possible to vary from manufacturer to manufacturer.
However both ABMA and ISO have published standards related to load ratings.
ABMA std. 9 - Load Ratings and Fatigue life for Ball Bearings
ABMA std. 12.1 and 12.2 - Instrument Ball Bearings
ISO 76 - Static Load Ratings
ISO 281- Dynamic Load Ratings and Rating Life.

With regard to load ratings, one must remember that static load ratings and dynamic load ratings are calculated on completely different ways and there is not direct relationship to one another.

The Basic Static Load Rating applies to bearings where motion does not occur or occurs only infrequently. The basic load ratings and calculation methods are based on methods described by the above-mentioned ISO recommendations.
As a standard of permissible static load, the basic load rating is specified as follows:

a) Maximum contact pressure at the contact point 4200 MPa (1 MPa=100 $N/cm^2$)
b) Total permanent deformation of the compressed zone can be, approximately, $1/10000^{th}$ of the rolling elementary diameter.
c) The basic load rating for stainless steel is 80% of that for standard bearing steel.

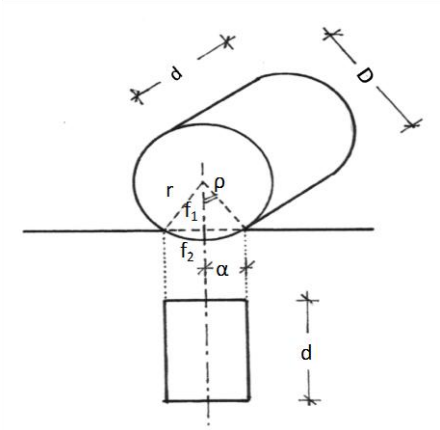


According to the above recommendations, one can proceed as follows (see Figure 21):

$$f_2 = \frac{2r}{10000} = r \cdot 2 \cdot 10^{-4} \quad \text{and} \quad f_1 = r - f_2 = 0.9998 \cdot r$$

From the above, we find: $\cos\rho = \frac{f_1}{r} = 0.9998 = \text{constant}$ or finally:

$$\rho = 0.020\,\text{rad}\,(\sim 1.146^o) = \text{constant}$$

From the sketch of Figure 21, we get:

$$\alpha \cong 2\pi r \frac{\rho}{2\pi} = \rho r$$

Therefore, for the safe undertaking of a load $T_o$, the required length d of the cylinder of Fig. 21, can be determined by the following relations:

$$d = \frac{T_o}{2\alpha\sigma_{per}}, \quad \text{or for stainless steel: } d = \frac{1.25 \cdot T_o}{2\alpha\sigma_{per}}$$

## 6.2 Selection of the appropriate C.R.P.B.

According to the results of §5.4, we select a device with R=1m, and D=2r=7cm. From §6.1, we have $\alpha = \rho r = 0.020 \cdot 3.5 = 0.07\,\text{cm}$ and

$$d = \frac{T_o}{2\alpha\sigma_{per}} = \frac{300000}{2 \cdot 0.07 \cdot 42000} = 51\text{cm}$$ or, equivalently, 4 cylinders with length 15cm.

The designed C.R.P.B. device shown in Fig. 22 can undertake loads acting to any direction because the rolling cylinders operate along two perpendicular axes.

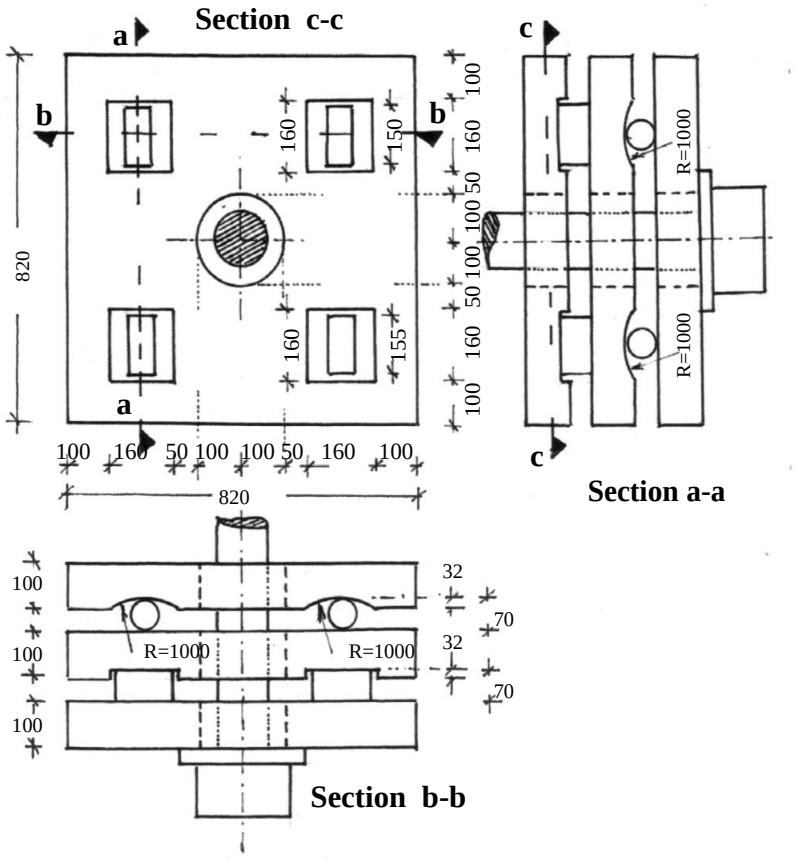


*Figure 22.* The required C.R.P.B.

## 7 CONCLUSIONS

In this paper, a movable anchorage system with Classical Rolling Pendulum Bearing (C.R.P.B.) for vibration control of stay cables has been proposed and investigated. A model for the control system has been formulated, based on the taut string representation in which the proposed device has been incorporated.
From the studied cases, one can conclude to the followings:

- The constant of the equivalent spring of the CRPB system has been assessed.
- The results of cable response show that the proposed CRPB device can effectively reduce the oscillation magnitude of the cable, proving the efficiency of the system.
- The observed decrease of the cable's oscillations amounts from 15% to 50%, while the motion of the anchor-head of the selected and designed device amounts from 1.5 to 6 cm. One must note that the CRPB device is very effective even for external loads acting with frequencies equal or near to one

of the eigenfrequencies of the strained cable.

- The design parameters of the CRPB system for the selected cables are identified and the proper device has been designed.
- The proposed anchorage system is shown to perform more efficiently than the conventional passive external dampers, presenting a better solution from aesthetics point of view.

## REFERENCES

[1] J.F. Fleming, "Non-linear static analysis of cable-stayed bridge structures", *Comp. Struct*., 1979, 10, pp. 986-1000

[2] C.F. Kollbruner, N. Hajdin, and B. Stipanic, "Contribution to the analysis of cable-stayed Bridges", *Inst. For Engineering Research Editions*, 1980, N. 48, Schulthess Verlag, Zürich

[3] D. Bruno, and A. Grimaldi, "Non-linear behavior of long-span cable-stayed bridges", *Meccanica, J. of the Italian Assoc. for Theoretical and Applied Mechanics (A/META)*, 1985, 20(4), pp. 303-313

[4] N. Gimsing, *Cable Supported Bridges – Concept and design*, 2nd Edition, John Wiley & Sons, Chichester, 1997

[5] M.S. Khalil, "Non-linear analysis of cable-stayed bridges at ultimate load level", *Canadian J. of Civil Engineering*, 1999, 23(5), pp. 1111-1117

[6] M. Virgoreux, "Recent evolution on cable-stayed bridges", *J. of Engineering Structures*, 1999, 21, pp. 737-755

[7] G.T Michaltsos, J.C. Ermopoulos, and T.G. Konstantakopoulos, "Preliminary design of cable-stayed bridges for vertical static loads", *J. of Structural Engineering and Mechanics*, 2003. 16(1), pp. 1-15

[8] A.M.S. Freire, J.H.O. Negrão, and A.V. Lopez, A.V. "Geometrical non-linearities on the static analysis of highly flexible steel cable-stayed bridges", *Computers & Structures*, 2006, 84(31-32), pp. 2128-2140

[9] J.F. Fleming, and E.A. Egeseli, "Dynamic behavior of a cable-stayed bridge", *Int. Journal of Earthquake Eng. & Structural Dynamics*, 1980, 8(1), pp. 1-16

[10] A.S. Nazmy, and A.M. Abdel-Ghaffar, "Non-linear earthquake response analysis of long-span cable-stayed bridges", *Earthquake Engineering and Structural Dynamics*, 1990, 19, pp. 45-62

[11] A.M. Abdel-Ghaffar, and M.A. Khalifa, "Importance of cable vibration in dynamics of cable-stayed bridges", *Journal of Engineering Mechanics*, 1991, 117(11), pp. 2571-2589

[12] D. Bruno, and V. Colotti, "Vibration analysis of cable-stayed bridges", *Journal of Structures Ing. International*, 1994, 1, pp. 23-28

[13] P.K. Chatterjee, T.K. Datta, and C.S. Suruna, "Vibration of cable-stayed bridges under moving vehicles", *Journal of Structures Ing. International*, 1994, 2, pp. 116-121

[14] G.T. Michaltsos, "A simplified model for the dynamic analysis of cable-stayed bridges", *Facta Universitatis*, 2001, 3(11), pp. 185-204

[15] T.G. Konstantakopoulos, G.T. Michaltsos, and D.S. Sophianopoulos, "A simplified model for the study of the lateral-torsional vibration of cable-stayed bridges", *Proceedings of the Eurodyn 2002*, Munich, 2002

[16] P.H. Wang, M.Y. Liu, Y.T. Huang, and L.C. Lin, "Influence of lateral motion of cable-stayed bridges", *Structural Engineering and Mechanics*, 2010, 34(6), pp. 719-738

[17] D.Q. Cao, M.T. Song, W.D. Zhu, R.W. Tucker, and C.H.-T. Wang, "Modeling and analysis of the in-plane vibration of a complex cable-stayed bridge", *J. of Sound and Vibration*, 2012, 331(26), pp. 5685-5714

[18] J.H.G. Macdonald, "Multi-modal vibration amplitudes of taut inclined cables due to direct and/or parametric excitation", *J. of Sound and Vibration*, 2016, 363, pp. 473-494

[19] I.G. Raftoyiannis, and G.T. Michaltsos, "Movable anchorage systems for vibration control of stay-cables in bridges", *Engineering Structures*, 2016, 112, pp. 162-171
[20] I.G. Raftoyiannis, and G.T. Michaltsos, "Curved-in-plane cable-stayed bridges. A mathematical model", *Int. Journal of Structural Stability and Dynamics*, 2012, 12(3), DOI: 10.1142/S0219455412500113
[21] J. Ermopoulos, A. Vlahinos, and Y.-C. Wang, "Stability analysis of cable-stayed bridges", *Comp. Structures*, 1992, 44(5), pp. 1083-1089
[22] A. Bosdogianni, and D. Olivari, "Wind-reduced and Rain-induced oscillations of cable-stayed bridges", *Journal of Wind Eng. and Industrial Aerodynamics*, 1997, 64(2-3), pp. 171-185
[23] G.T. Michaltsos, "Stability of a cable-stayed bridge's pylon, under time-depended loading", *Collection of papers in memory of Academician P.S. Theocharis*. Inst. of Mechanics Problems and Academy of Sciences, Russia, Inst. of Mechanics of Nat. Acad. of Sciences, Armenia, 2005
[24] G.T. Michaltsos, I.G. Raftoyiannis, and T.G. Konstantakopoulos, "Dynamic Stability of cable-stayed bridge pylons", *Int. Journal of Structural Stability and Dynamics*, 2008, 8(4), pp. 627-643
[25] J.O. Pedro, and A.J. Reis, "Non-linear analysis of composite steel-concrete cable-stayed bridges", *Engineering Structures*, 2010, 32(9), pp. 2702-2716
[26] Y. Hikami, and N. Shiraishi, "Rain-wind-induced vibrations of cables in cable stayed bridges", *Journal of Wind Engineering and Industrial Aerodynamics*, 1988, 29(1-3), pp. 409-418
[27] Y. Achkire, and A. Preumont, "Active tendon control of cable-stayed bridges", *J. of Earthquake Engineering & Structural Dynamics*, 1996, 25(6), pp. 585-597
[28] J.H.G. Macdonald, E.L. Dagless, B.T. Thomas, and C.A. Taylor, "Dynamic measurements of the Second Severn Crossing", *Proceedings of the Institution of Civil Engineers – Transpor*t, 1997, 123(4), pp. 241-248
[29] K. Wilde, and W. Witkowski, "Simple model of rain-wind-induced vibrations of stayed cables", *Journal of Wind Engineering and Industrial Aerodynamics*, 2003, 91(7), pp. 873-891
[30] R.A. Ibrahim, "Nonlinear vibrations of suspended cables – Part III: Random excitation and interaction with fluid flow", *Applied Mechanics Reviews*, 2004, 57(6), pp. 515-549
[31] D. Sophianopoulos, "Rain-wind induced vibrations in stay cables – Response characteristics, excitation mechanism and modeling." *Int. Journal of Bridge Engineering*, 2013, 1(1), pp. 29-36
[32] J. Touaillon, *Improvement in Buildings*, U.S. Patent Office, Letters Patent No.99973, USA, 1870.